Selective lymphodepletion underlies the efficacy of horse anti-thymocyte globulin-based immunosuppressive therapy in aplastic anemia

Emma S. Pool,[1] Cilia R. Pothast,[1] Shannah M. Gennesse,[1] Esther H.M. van Egmond,[1] Julia M. Giezen,[2] Sabrina A.J. Veld,[1] René E.M. Toes,[2] Frits Koning,[3] Constantijn J.M. Halkes,[1] Mirjam H.M. Heemskerk,[1] Dirk Jan A.R. Moes[4] and Jennifer M-L. Tjon[1]

[1]Department of Hematology; [2]Department of Rheumatology; [3]Department of Immunology and [4]Department of Clinical Pharmacy and Toxicology, Leiden University Medical Center, Leiden, the Netherlands

Correspondence: Jennifer M-L. Tjon
j.m.l.tjon@lumc.nl

Received: October 3, 2025.
Accepted: January 21, 2026.
Early view: January 29, 2026.

https://doi.org/10.3324/haematol.2025.300002

Abstract

Horse-derived anti-thymocyte globulin (ATGAM) in combination with long-term ciclosporin is the first-line treatment for most immune-mediated aplastic anemia (AA) patients. The exact impact of this immunosuppressive therapy (IST) on hematologic recovery and the immune landscape, however, remains poorly understood. We report a longitudinal analysis of the pharmacodynamic effects of ATGAM-based IST in a cohort of 44 AA patients. We used flow cytometry to quantify plasma levels of lymphocyte-binding ATGAM, which is believed to mediate the therapeutic effect. Population pharmacokinetic modeling revealed substantial between-patient variability in ATGAM exposure, with higher exposure levels associating with earlier hematologic recovery. ATGAM bound all lymphoid lineages and profoundly depleted T and natural killer cells at high plasma concentrations. Strikingly, ATGAM did not deplete B cells but instead induced an increase in $CD27^+$ B cells. Deep immunophenotyping on series of peripheral blood samples collected up to three years after start of IST demonstrated that ATGAM induced rapid depletion of T cells, including $KLRG1^+$ terminally differentiated $CD8^+$ T cells and Th17-like $CCR6^+CD4^+$ T cells. Although naïve and pathogen-specific T cells were also depleted, they recovered quickly, indicating preservation of protective immunity. Notably, $CCR6^{++}$ B cells, implicated in AA pathogenesis, escaped ATGAM depletion but reduced gradually over time along with residual potentially pathogenic T cells, including the $CCR6^+CD4^+$ T cells. This could explain the crucial contribution of long-term ciclosporin to successful IST. Collectively, our results identify ATGAM exposure as a factor influencing hematologic recovery and indicate that the therapeutic effect of IST goes beyond total lymphodepletion but is rather the result of selective depletion and suppression of key lymphocyte subpopulations.

Introduction

Immune-mediated aplastic anemia (AA) is a bone marrow failure syndrome caused by an autoimmune attack on the hematopoietic stem and progenitor cells (HSPC).[1] The resulting peripheral cytopenias can lead to severe bleeding and infections. Effective treatments are allogeneic hematopoietic stem cell transplantation or immunosuppressive therapy (IST). IST is the first-line treatment for most patients due to older age or lack of a matched donor.[2]

Standard first-line IST for AA combines anti-thymocyte globulin (ATG) with long-term ciclosporin. ATG is a polyclonal antibody mixture that can be produced by immunizing horses or rabbits with human thymocytes. In AA, both horse-derived ATG (ATGAM®, Pfizer) and rabbit-derived ATG (Thymoglobulin®, Sanofi) have been applied. However, ATGAM is preferred since it results in superior response rates and overall survival.[3,4] Approximately 70% of patients show hematologic recovery after ATGAM-based IST, with a gradual improvement in peripheral blood counts over several months.[2,4,5]

The pharmacodynamics of ATGAM-based IST are poorly understood. Its therapeutic effect is attributed to the depletion of autoreactive immune cells implicated in AA pathogenesis. ATGAM, administered at 40 mg/kg/day for four consecutive days,[2] is thought to induce immediate lymphodepletion, possibly through complement-dependent lysis or activation-induced apoptosis.[6,7] Subsequently, long-term ciclosporin is believed to suppress residual and reconstituted lymphocytes through calcineurin and IL-2 blockade.[8,9] Since

ATGAM is manufactured in horses, it contains antibodies against both non-human and human antigens. Therefore, only a small 'active' fraction can bind human immune cells and mediate its immunomodulatory effects. The precise specificities of this active ATGAM fraction are unknown and its activity differs from the more extensively studied rabbit-derived ATG;[7,10] however, ATGAM has been shown to bind a spectrum of proteins on the surface of immune cells,[11,12] and to reduce $CD4^+$, $CD8^+$ and regulatory T cells *in vivo*.[4,13] Similarly, the relationship between active ATGAM exposure and lymphodepletion is unclear, and the impact of ATGAM plus ciclosporin on the immune landscape has not been characterized in detail. Previously, we identified potentially pathogenic T- and B-cell subpopulations in AA patients.[14,15] These $CCR6^{++}$ B cells, Th17-like $CCR6^+CD4^+$ T cells and $KLRG1^+$ terminally differentiated $CD8^+$ T cells were enriched at diagnosis, co-localized in bone marrow, and were significantly reduced at six months post ATGAM. This decrease could imply that IST selectively depletes specific lymphocyte subpopulations.

In this study, we aimed to identify the effects of ATGAM exposure on hematologic recovery in 44 AA patients. For the first time, we quantified active ATGAM concentrations in patient plasma using flow cytometry, and applied population pharmacokinetic (POPPK) modeling to estimate exposure. Furthermore, to elucidate the impact of IST with ATGAM plus ciclosporin on the immune landscape, we performed spectral flow cytometry on peripheral blood samples collected before and at multiple time points after start of IST. Our results present active ATGAM exposure as a factor influencing hematologic recovery and reveal that successful IST involves selective removal and suppression of key lymphocyte subpopulations rather than a full immune 'reset'.

Methods

Patients and plasma samples

Plasma samples (N=381) were collected from 44 treatment-naïve AA patients before each ATGAM infusion and up to 82 days after the first infusion (median 9, range 4-13 samples/patient). Peripheral blood mononuclear cells (PBMC) were collected from 3 of 44 patients at diagnosis and up to 3.5 years post ATGAM (7-10 samples/patient), and 5 healthy donors. Patients' characteristics are listed in Table 1. Patients <40 years of age were screened for Fanconi anemia to exclude congenital bone marrow failure. Patients received IST according to Dutch guidelines: four consecutive days 40 mg/kg/day ATGAM and 5 mg/kg/day ciclosporin for at least six months.[16] Exceptions were patients (two days ATGAM), UPN9 (four days ATGAM with two-day break after infusion two), and UPN46 (118 days ciclosporin). ATGAM was administered intravenously over 12 hours. Nineteen of 44 patients responded within six months after start of IST, which was defined as becoming transfusion-independent and a neutrophil count of $\geq 0.5 \times 10^9$/L.[2] Plasma or PBMC were stored at -80°C or -196°C until bioanalysis, respectively. This study was ap-

Table 1. Patients' characteristics.

Characteristic	Patients N=44
Age at diagnosis, years, median (range)	54 (20-79)
Sex, N	
Male	26
Female	18
Weight at diagnosis, Kg, median (range)	80 (51-120)
BMI at diagnosis, median (range)	24.7 (17.6-34.3)
Height at diagnosis, cm, median (range)	176 (156-198)
Severity of disease at diagnosis, N	
Non-severe AA	7
Severe AA	23
Very severe AA	14
Total lymphocyte count pre-ATGAM, $x10^6$/L, median (range)*#	1375 (260-2,890)
$CD4^+$ T-cell count pre-ATGAM, $x10^6$/L, median (range)*#	732 (21-1,479)
$CD8^+$ T-cell count pre-ATGAM, $x10^6$/L, median (range)*#	363 (71-949)
NK-cell count pre-ATGAM, $x10^6$/L, median (range)*#	77 (4-291)
B-cell count pre-ATGAM, $x10^6$/L, median (range)*	124 (17-631)
Response to IST 6 months post-ATGAM, N	
Non-response	21
Partial response	14
Complete response	5
Unknown (died <6 months after first ATGAM infusion)	4

AA: aplastic anemia; ATGAM: horse-derived anti-thymocyte globulin (ATGAM®); BMI: Body Mass Index; IST: immunosuppressive therapy;NK: natural killer. *Cell counts between days -2 to 0 pre-ATGAM infusion. #Data missing for 2 patients.

proved by the Medical Ethical Committee of the Leiden University Medical Center (B21.003).

ATGAM measurement and spectral flow cytometry

Flow cytometry was used to quantify active ATGAM concentrations in plasma, and to perform deep immunophenotyping in peripheral blood. For active ATGAM measurement, cryopreserved PBMC from a single healthy donor were incubated with serial dilutions of patient plasma using a protocol based on a previously validated assay for quantifying lymphocyte-binding antibody concentrations,[17] and stained with a six-marker antibody panel including anti-horse IgG. Subsequently, cells were measured by flow cytometry, and active ATGAM plasma concentrations were determined. For deep phenotyping of lymphocytes, cryopreserved PBMC samples were stained with a 25-marker panel (*Online Supplementary Table S1*), measured by spectral flow cytometry, and analyzed by dimensionality reduction.[18] A detailed description of all methods used, including the quantification of total ATGAM in plasma by ELISA, is provided in the *Online Supplementary Methods* and *Online Supplementary Figures S1-S3*.

Exposure-response analyses

Population pharmacokinetic modeling (POPPK) was performed in NONMEM® to estimate ATGAM exposure as detailed in the *Online Supplementary Methods*, *Online Supplementary Tables S2, S3*, and *Online Supplementary Figure S4*. Downstream exposure-response analyses used clinical data collected until day 180, because IST-response is assessed 3-6 months post ATGAM.[2] As a measure for hematologic recovery, we evaluated peripheral blood neutrophil and reticulocyte counts from routine measurements, generally taken at least weekly. Thrombocyte and hemoglobulin levels were not analyzed to avoid potential bias caused by blood transfusions. To study lymphodepletion and immune reconstitution, we analyzed peripheral blood lymphocyte counts from routine measurements, typically collected once every two weeks. To correct for missing immune reconstitution data, non-linear mixed effect modeling was performed using SAEMIX.[19] (See the *Online Supplementary Methods* and *Online Supplementary Figure S5*.) Data visualization and statistical analyses were performed in R v4.4.1 (Rstudio v2023.03) using Mann-Whitney *U* test for continuous variables, Fisher's Exact test for categorical variables, and Spearman's correlation tests. $P \leq 0.05$ was considered statistically significant.

Results

Active ATGAM binds all major lymphoid lineages

To study the effects of ATGAM, the concentration of ATGAM capable of binding PBMC from an unrelated healthy donor (active ATGAM hereafter) was quantified in plasma from 44 adult AA patients using flow cytometry (Figure 1A). In patients that received the standard regimen of four consecutive days 40 mg/kg/day ATGAM, active ATGAM concentrations increased over the four days of infusion and reached a median peak concentration of 131 AU/mL on day 4 (Figure 1B). After the last infusion, concentrations rapidly decreased, and typically fell below the concentration of 10 AU/mL by day 20. The pharmacokinetics of active ATGAM varied considerably between patients in both peak concentrations (range 31-497 AU/mL on day 4) and clearance rates (Figure 1B). Similar variability was observed in total ATGAM concentrations (e.g., active ATGAM and ATGAM binding to other [non]-human targets combined) quantified in the same plasma samples using ELISA (*Online Supplementary Figure S6A*). Active ATGAM in patient plasma was detected on donor T, natural killer (NK) and B cells. However, pharmacokinetics differed as B-cell binding active ATGAM was detected longer than T- or NK-cell binding active ATGAM (Figure 1C, *Online Supplementary Figure S6B*).

Active ATGAM exposure is increased in aplastic anemia patients with higher body weight

Given the variability in active ATGAM concentrations between patients, POPPK modeling was performed to estimate the full concentration-time curve of active ATGAM exposure. The POPPK of intravenously administered active ATGAM were best described by a two-compartment model with first-order linear elimination (*Online Supplementary Figure S7*). This model showed adequate agreement between observed and model-estimated active ATGAM concentrations (*Online Supplementary Figures S8, S9*). Exposure (AUC0-inf) was defined as the estimated area under the concentration-time curve (*Online Supplementary Table S4*). Since this study is the first to report on active ATGAM, we also validated the accuracy of our approach by performing POPPK modeling for total ATGAM (*Online Supplementary Table S5, Online Supplementary Figures S10, S11*) to simulate the dosing regimens described in the manufacturer's brochure.[20] This revealed strong agreement between model-estimated and reported total ATGAM concentrations for an external cohort of AA patients (*Online Supplementary Figure S12*).

To identify factors driving between-patient variability in active ATGAM pharmacokinetics, the impact of clinical covariates was evaluated. No significant effects of sex, age and lymphocyte counts pre-ATGAM were observed (*Online Supplementary Figure S13*). Since ATGAM dose is based on body weight, we anticipated clearance to increase with body weight to obtain similar ATGAM exposures across patients. However, we found that patients with higher body weights had higher active ATGAM concentrations in time, resulting in higher exposures (Figure 1D), as neither clearance nor volume of distribution were influenced by weight (Figure 1E, F).

Higher active ATGAM exposure associates with earlier hematologic recovery

To investigate the effect of active ATGAM exposure on hematologic recovery, patients were categorized into low, medium and high exposure groups based on the exposure tertiles of 1,515 and 2,216 AU/day/L (Figure 2A). Neutrophil and reticulocyte counts served as a measure for bone marrow recovery. The data of two patients in the low-exposure group, one patient in the medium-exposure group, and one in the high-exposure group were censored before day 180 because of death. There was no significant difference in age, sex, disease severity, eltrombopag use and ciclosporin

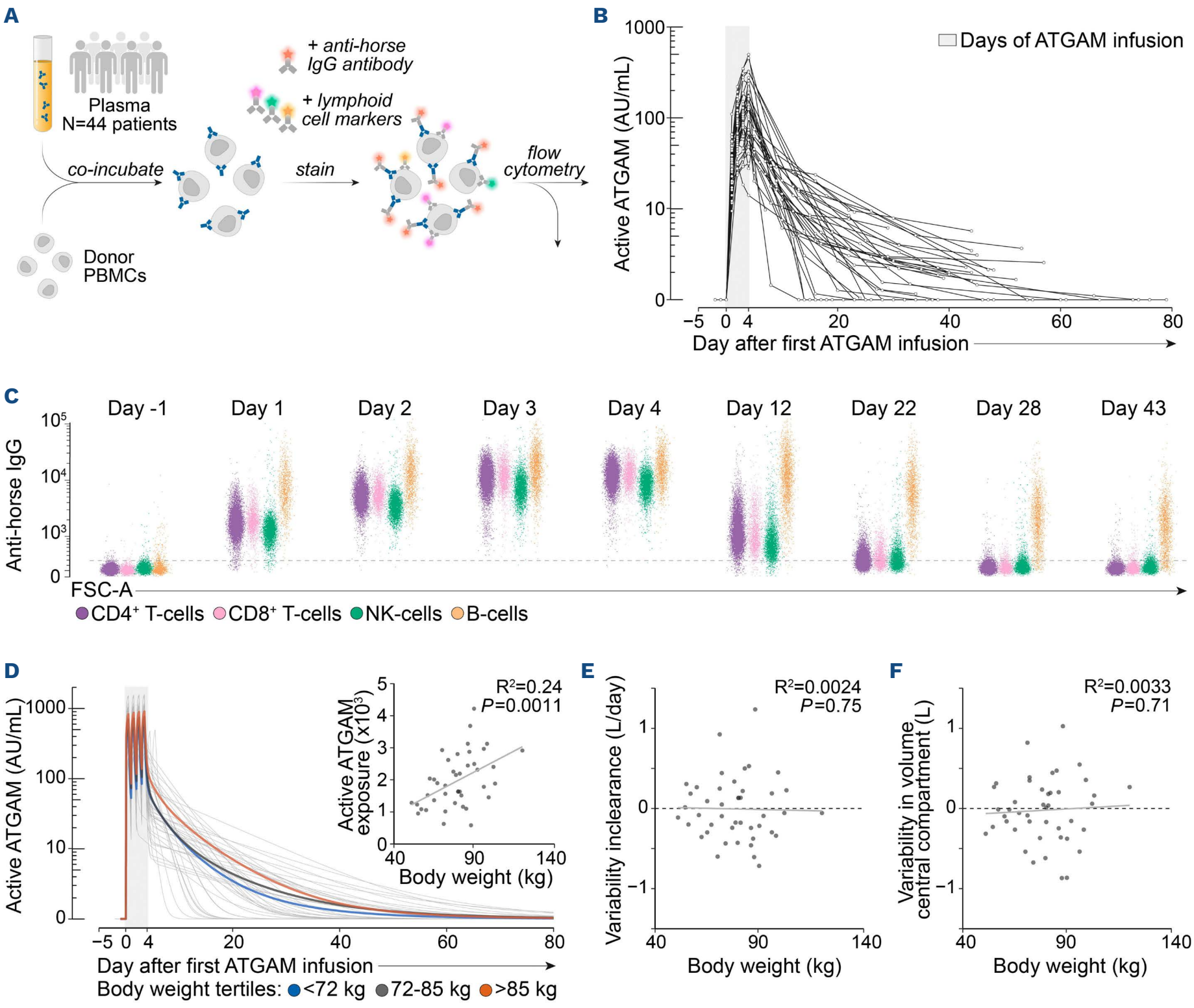

Figure 1. Active ATGAM binding specificities and concentration-time profiles in plasma from aplastic anemia patients. (A) Experimental approach. Donor peripheral blood mononuclear cells (PBMC) were incubated with plasma samples collected pre- and post-infusion of horse-derived anti-thymocyte globulin (ATG; ATGAM®), stained and analyzed by flow cytometry to determine the plasma levels of free active ATGAM capable of binding to human lymphocyte lineages. (B) Measured active ATGAM levels in patient plasma (in arbitrary units/mL; N=44 patients) in time before, during and after ATGAM infusion on days 0-4. (C) Flow cytometric plots demonstrating the binding of active ATGAM in plasma from a representative patient (UPN33) to CD4⁺ T cells, CD8⁺ T cells, natural killer (NK) cells or B cells from a healthy donor, measured using an Alexa Fluor 488-conjugated anti-horse IgG antibody. (D) Model-estimated active ATGAM plasma concentrations over time before, during and after ATGAM infusion on days 0-4. Mean active ATGAM concentrations are presented for patients within the lowest (blue), medium (yellow), and highest (red) body weight quantiles, who received four consecutive days 40 mg/kg/day ATGAM. Insert: correlation between model-estimated active ATGAM exposure and body weight. (E and F) Covariate plots showing the relationship between body weight and the inter-individual variability in estimated active ATGAM clearance (E) or volume of distribution (F). Each dot represents one patient. Only patients that received the standard dosing regimen of four consecutive days 40 mg/kg/day ATGAM are shown.

discontinuation between the groups, and none of the patients started second-line treatment before day 180 (*Online Supplementary Table S6*). In all three exposure groups, neutrophil and reticulocyte counts gradually increased post-ATGAM (Figure 2B, C). Reticulocyte counts peaked in a few patients within the first 120 days post-ATGAM. Notably, the high- and medium-exposure groups tended to have higher neutrophil and reticulocyte counts from day 60 onward, despite similar baseline counts compared to the low-exposure group (Figure 2B, C). This difference was most pronounced around day 90 (Figure 2B, C) and diminished 180 days post-ATGAM infusion, suggesting that increased active ATGAM exposure associates with earlier hematologic recovery but does not impact 6-month response rates.

ATGAM induces profound depletion of T and natural killer cells but not of B cells

As we showed that ATGAM binds all major lymphoid lineages, we studied the response of active ATGAM exposure on T-, NK- and B-cell counts in peripheral blood. To correct for missing immune reconstitution data, total lymphocyte, T- and NK-cell counts were estimated by non-linear mixed modeling. ATGAM induced a strong reduction in $CD4^+$ T cells, $CD8^+$ T cells and NK cells, with no differences between the active ATGAM exposure groups (Figure 2D). Depletion of these lineages was short-lived and only observed immediately post-infusion, suggesting that T- and NK-cell depletion requires a minimal active ATGAM plasma concentration (+/-100 AU/mL, estimated

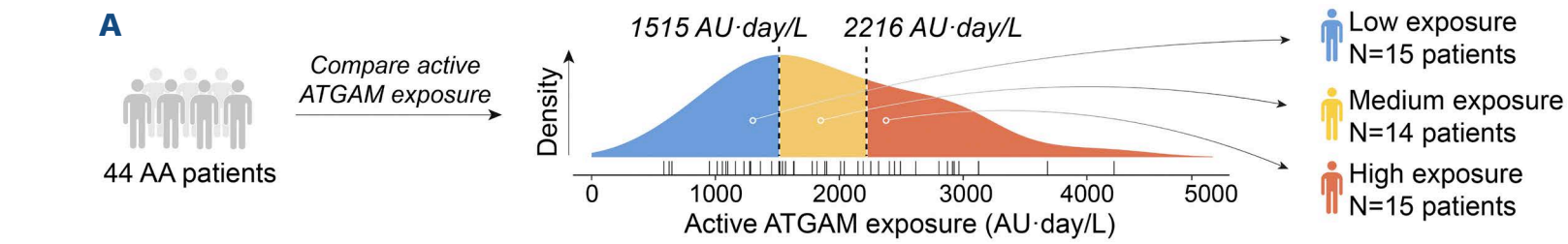

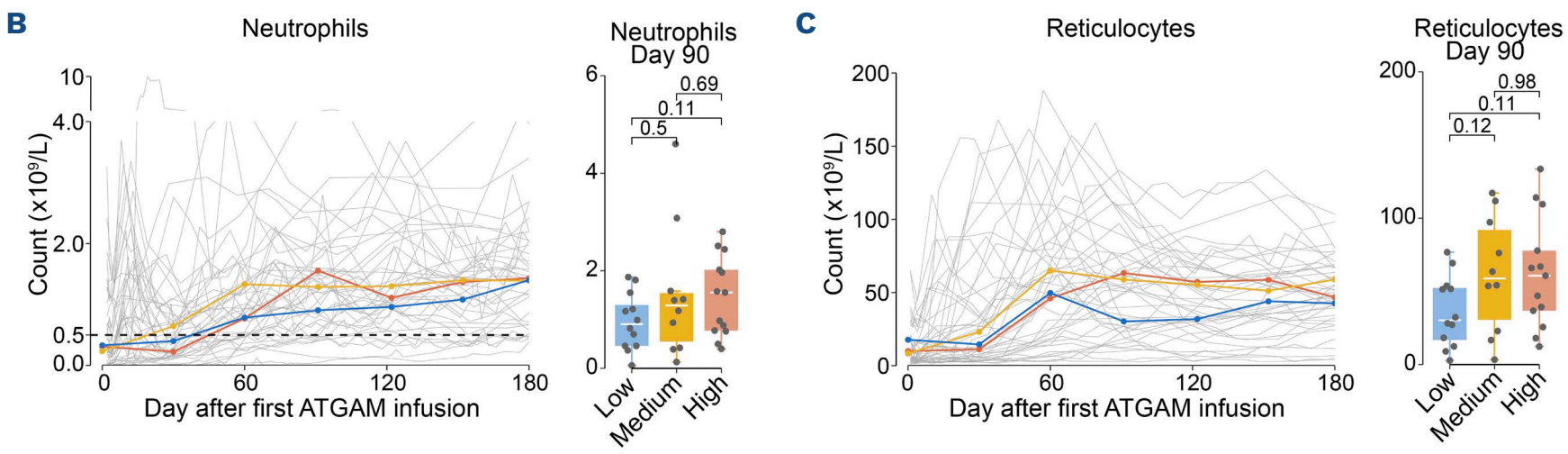

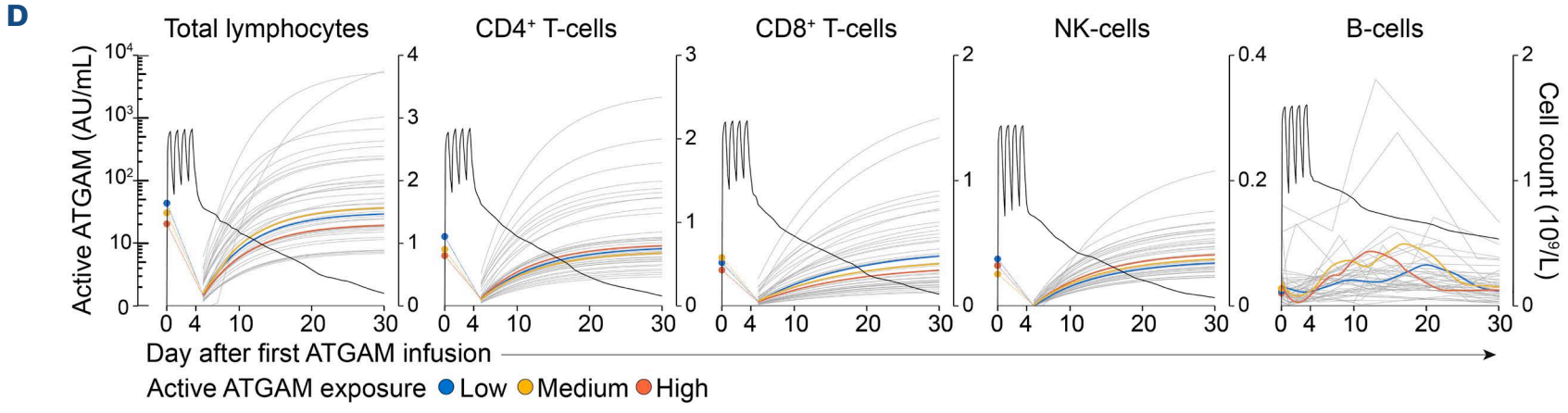

Figure 2. Impact of active ATGAM exposure on peripheral blood counts. (A) Histogram showing the distribution of active horse-derived anti-thymocyte globulin (ATG; ATGAM®) exposure across the patient cohort. (B and C) Absolute neutrophil (B) and reticulocyte (C) counts over time up to 180 days after ATGAM infusion on days 0-4. Light gray lines present individual patients. Blue, yellow and red lines present group medians of low, medium and high active ATGAM exposure groups, on days 0, 30, 60, 91, 122, 152 and 180 +/- 7 days, respectively. Cell counts were unavailable for 2 (day 30), 5 (day 60), 9 (day 91), 9 (day 122), 7 (day 152) and 9 (day 180) patients divided across all exposure groups. Box plots represent the group median, whiskers represent 1.5 * interquartile range. (D) Median model-estimated active ATGAM concentrations capable of binding to all lymphocytes, $CD4^+$ T cells, $CD8^+$ T cells, natural killer (NK) cells or B-cell plotted against absolute total lymphocyte, $CD4^+$ T-cell, $CD8^+$ T-cell, NK-cell or B-cell counts, respectively. Light gray lines present cell counts of individual patients. Blue, yellow and red lines present median cell counts of low, medium and high active ATGAM exposure groups, respectively. Model-estimated lymphocyte, $CD4^+$ T-cell, $CD8^+$ T-cell, NK-cell counts are presented, whereas observed B-cell counts are shown. AA: aplastic anemia.

from Figure 2D). Strikingly, B-cell counts did not show a consistent trend between patients post-ATGAM and, therefore, could not be modeled. Interestingly, B-cell counts even peaked post-ATGAM before returning to baseline around day 30, indicating that although ATGAM binds all lymphoid lineages, it exerts differential effects among different cell types.

Detection of ATGAM on patient lymphocytes confirms B-cell binding *in vivo*

To study the paradox that ATGAM binds donor B cells but does not induce B-cell depletion, we investigated the presence of ATGAM directly bound to patient PBMC. Unique series of PBMC samples collected from 3 AA patients before and immediately after ATGAM infusion were studied. A 25-marker spectral flow cytometry panel including

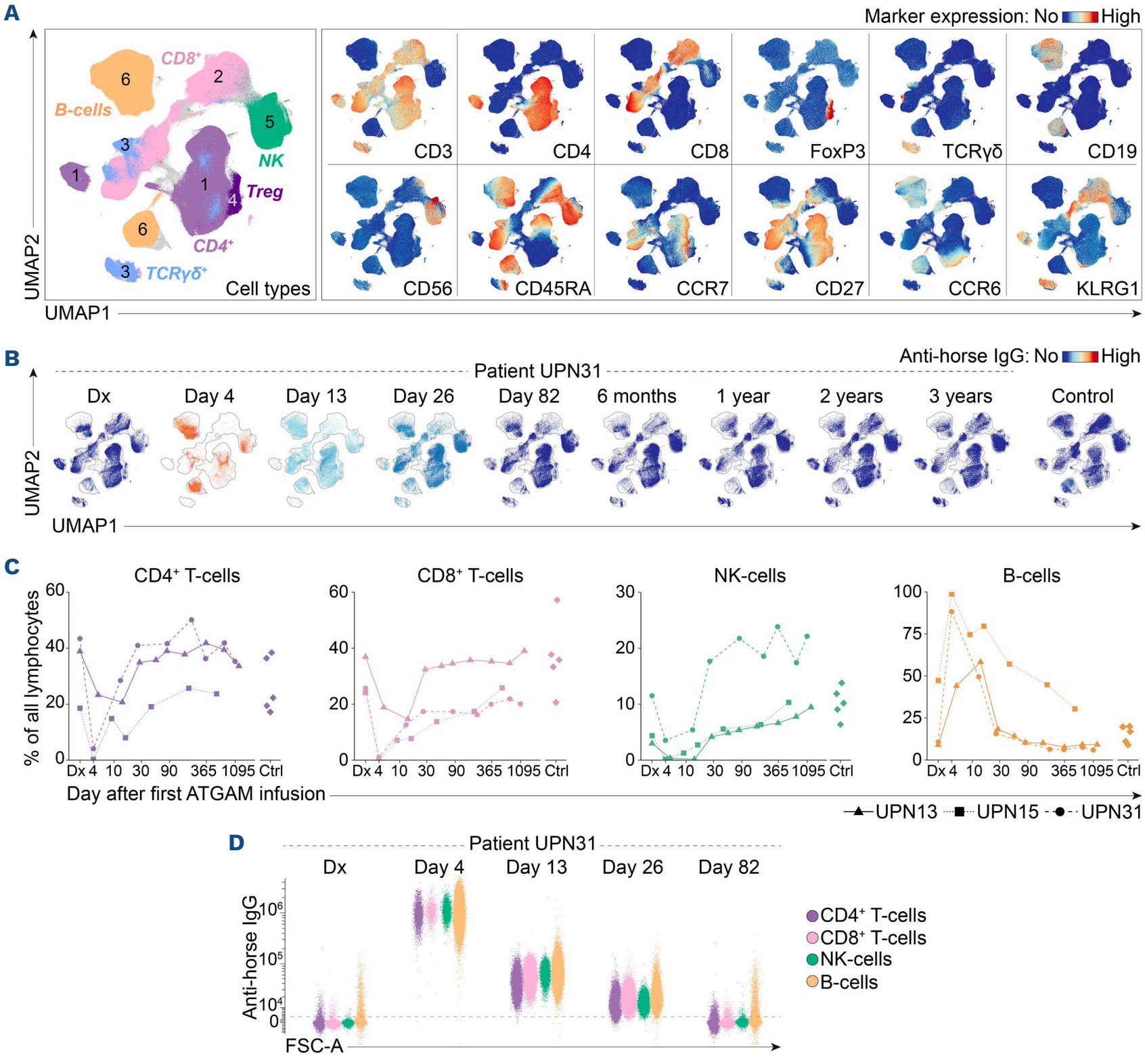

Figure 3. Binding of ATGAM and the impact of ATGAM-based immunosuppressive therapy on lymphocytes from aplastic anemia patients. (A) 3x10⁶ single, live lymphocytes downsampled from all peripheral blood mononuclear cells (PBMC) samples (UPN13, UPN15, UPN31 and 5 controls) visualized using an Uniform Manifold Approximation and Projection (UMAP) analysis. Colors indicate major lymphoid lineages or marker expression values. (B) UMAP plots showing the cellular composition of the lymphoid compartment in peripheral blood from UPN31 before and over time following horse-derived anti-thymocyte globulin (ATG; ATGAM®) infusion on days 0-4. The signal of the Alexa Fluor 488-conjugated anti-horse IgG antibody is shown. 0.1x10⁶ single, live lymphocytes are shown per time point. (C) Frequencies of major lymphoid lineages, shown as a percentage of all single, live lymphocytes per time point. Each line represents an individual patient. (D) Flow cytometry plots visualizing the presence of ATGAM directly bound to T, natural killer (NK) or B cells from UPN31 over time, detected using an Alexa Fluor 488-conjugated anti-horse IgG antibody incorporated into the spectral flow cytometry panel.

anti-horse IgG enabled the detection of ATGAM on the surface of in-depth phenotyped lymphocytes. To study the long-term effects of ATGAM plus ciclosporin, samples collected up to 3.5 years post-ATGAM were also analyzed (total of 7-10 samples/patient). Patients received 40 mg/kg/day ATGAM on four consecutive days, responded to IST (*Online Supplementary Figure S14*), and were cytomegalovirus (CMV) seropositive. Ciclosporin was discontinued after tapering two years post-ATGAM in Patient UPN31, and three years post-ATGAM in UPN13 and UPN15. As a reference, PBMC from 5 age-, sex- and CMV status-matched healthy donors were included.

To directly compare the immune landscape between time points, UMAP were generated after downsampling $0.1x10^6$ single, live lymphocytes from each sample (Figure 3A). The following major lymphoid lineages were identified: 1) $CD3^+CD4^+$ T cells; 2) $CD3^+CD8^+$ T cells; 3) $CD3^+TCR\gamma\delta^+$ T cells; 4) $CD3^+CD4^+FoxP3^+$ regulatory T cells; 5) $CD3^-CD56^+$ NK cells; and 6) $CD19^+$ B cells. Visualization of all samples from a representative patient in the UMAP revealed a shift in the lymphoid compartment over time, with the most obvious changes observed immediately after the last ATGAM infusion on day 4, when T and NK cells were reduced but B cells were still present (Figure 3B).

Quantification of lineage frequencies confirmed the presence of the major lymphoid lineages at AA diagnosis, with some heterogeneity between patients and no considerable differences compared to controls (Figure 3C, *Online Supplementary Figure S15A*). Immediately after the last ATGAM infusion (day 4/5) the composition of the lymphoid compartment changed dramatically. In agreement with previous observations, percentages of $CD4^+$, $CD8^+$, $TCR\gamma\delta^+$ and regulatory T and NK cells decreased in all patients, whereas B-cell frequencies increased. A trend towards normalization was observed from two weeks post-ATGAM onwards. Normalization of the lymphoid compartment continued up to six months post-ATGAM.

With anti-horse IgG, ATGAM was best detectable on day 4, and could be detected until day 26 on all circulating lymphocytes from the representative patient post-infusion (Figure 3B, D). There was no difference in the amount of ATGAM bound to T or B cells (*Online Supplementary Figure S15B*). To rule out a potential influence of ATGAM Fc-binding to the Fc-receptor on B cells, Fc-receptor blockade experiments were performed and no Fc-binding was found (*Online Supplementary Figure S16*). ATGAM binding to patient lymphocytes gradually decreased within one month post-infusion. Lower concentrations of ATGAM

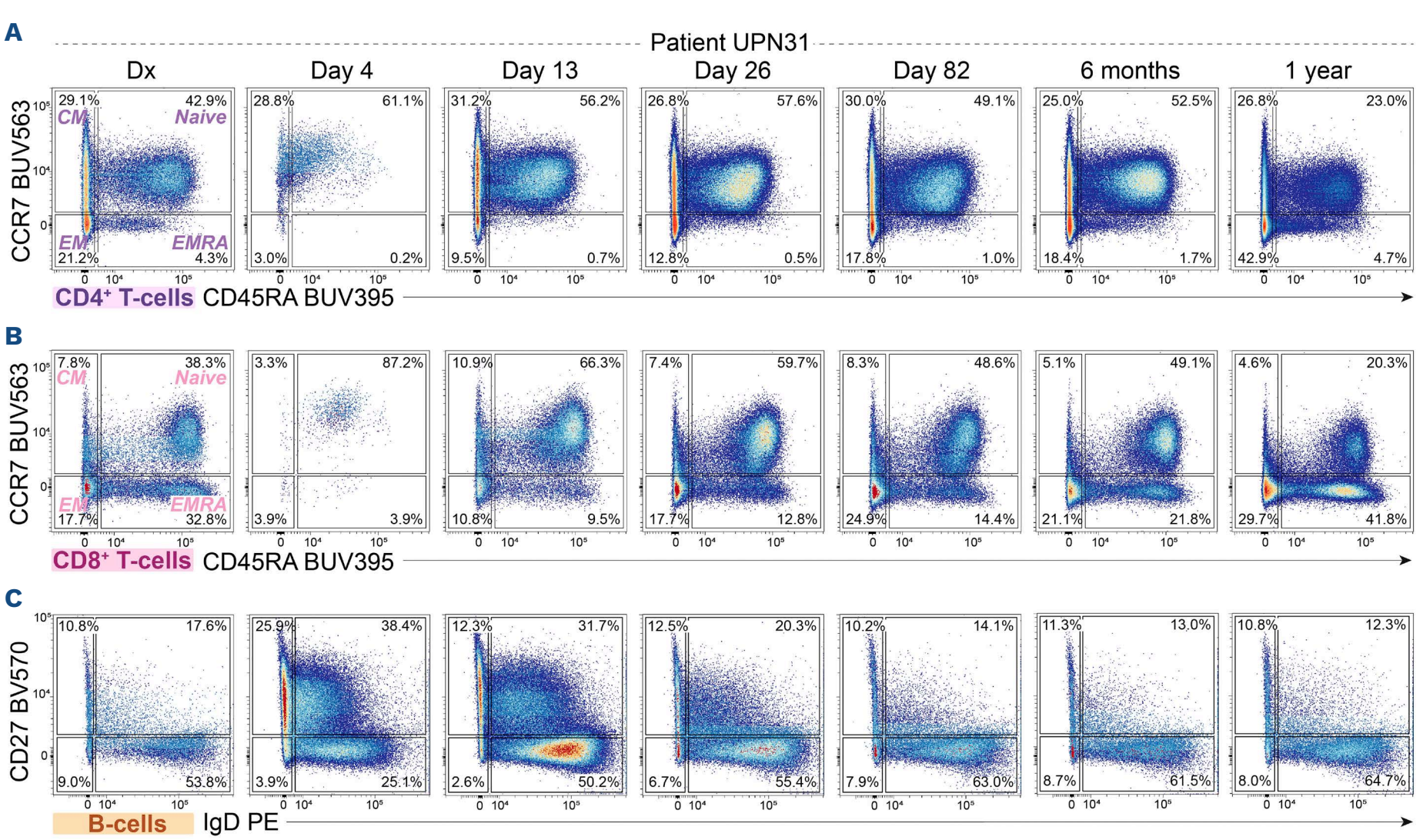

Figure 4. Impact of ATGAM-based immunosuppressive therapy at the immune subpopulation level in a representative aplastic anemia patient. (A-C) Flow cytometry plots visualizing the composition of the (A) $CD4^+$ T-cell compartment, (B) $CD8^+$ T-cell compartment, and (C) B-cell compartment from patient UPN31 before and over time following start of horse-derived anti-thymocyte globulin (ATG; ATGAM®)-based immunosuppressive therapy (IST) on day 0. CM: central memory, EM: effector memory; EMRA: terminally differentiated effector memory.

again correlated with T- and NK-cell recovery from two weeks post-infusion onwards. These findings confirm that while ATGAM binds to all lymphoid lineages, it does not induce B-cell depletion to the same extent as observed in T and NK cells.

ATGAM profoundly depletes memory T cells but induces an increase in CD27⁺ B cells

Next, we studied the immediate effects of ATGAM and long-term impact of ATGAM plus ciclosporin at the immune subpopulation level. In the representative patient, we observed a more profound decrease in memory T cells compared to naïve T cells post-ATGAM, with the strongest depletion of $CD45RA^{+}CCR7^{-}$ terminally differentiated effector memory (EMRA) $CD8^{+}$ T cells (Figure 4A, B, *Online Supplementary Figure S15C, D*). In contrast, we observed a striking increase in memory $CD27^{+}$ B cells immediately post-ATGAM (Figure 4C, *Online Supplementary Figure S15E*). The profound depletion of memory T cells and increase in memory $CD27^{+}$ B cells was observable across all patients post-ATGAM (Figure 5A-C). Only in patient UPN15 did memory T-cell frequencies remain high, which was attributable to the low number of T cells analyzed, as this patient experienced the strongest T-cell depletion (Figure 3C). Within two weeks post-ATGAM, both memory T cells and $CD27^{+}$ B-cell frequencies showed a trend towards normalization (Figure 5A-C). Notably, this normalization occurred independently of T- and B-cell proliferation, indicating that recovery was not driven by proliferation of remaining circulating cells (*Online Supplementary Figure S17*).

To further characterize the increase in $CD27^{+}$ B cells, we examined the identity of these cells in patient UPN31 on day 13 using a B-cell-oriented spectral flow cytometry panel. This revealed that the $CD27^{+}$ B cells comprised a heterogeneous population of both unswitched ($IgM^{+}IgD^{+}$) and switched (IgG^{+}, IgA^{+}) memory B cells (Figure 5D). Compared to healthy controls, these cells preserved high levels of CD21 and CD24, compatible with a resting B-cell state (Figure 5E). Additionally, they did not differentially express the activation markers CD80, CD86 and CD95 or complement inhibitors CD46 and CD55 (Figure 5E, F), illustrating that the increase in $CD27^{+}$ B cells is not the result of cell expansion or resistance to complement-mediated lysis. Consistent with these findings, the $CD27^{+}$ B cells harbored tetanus-specific cells, indicating their increase was driven by a recruitment of resting, pre-existing memory B cells in circulation (Figure 5G).

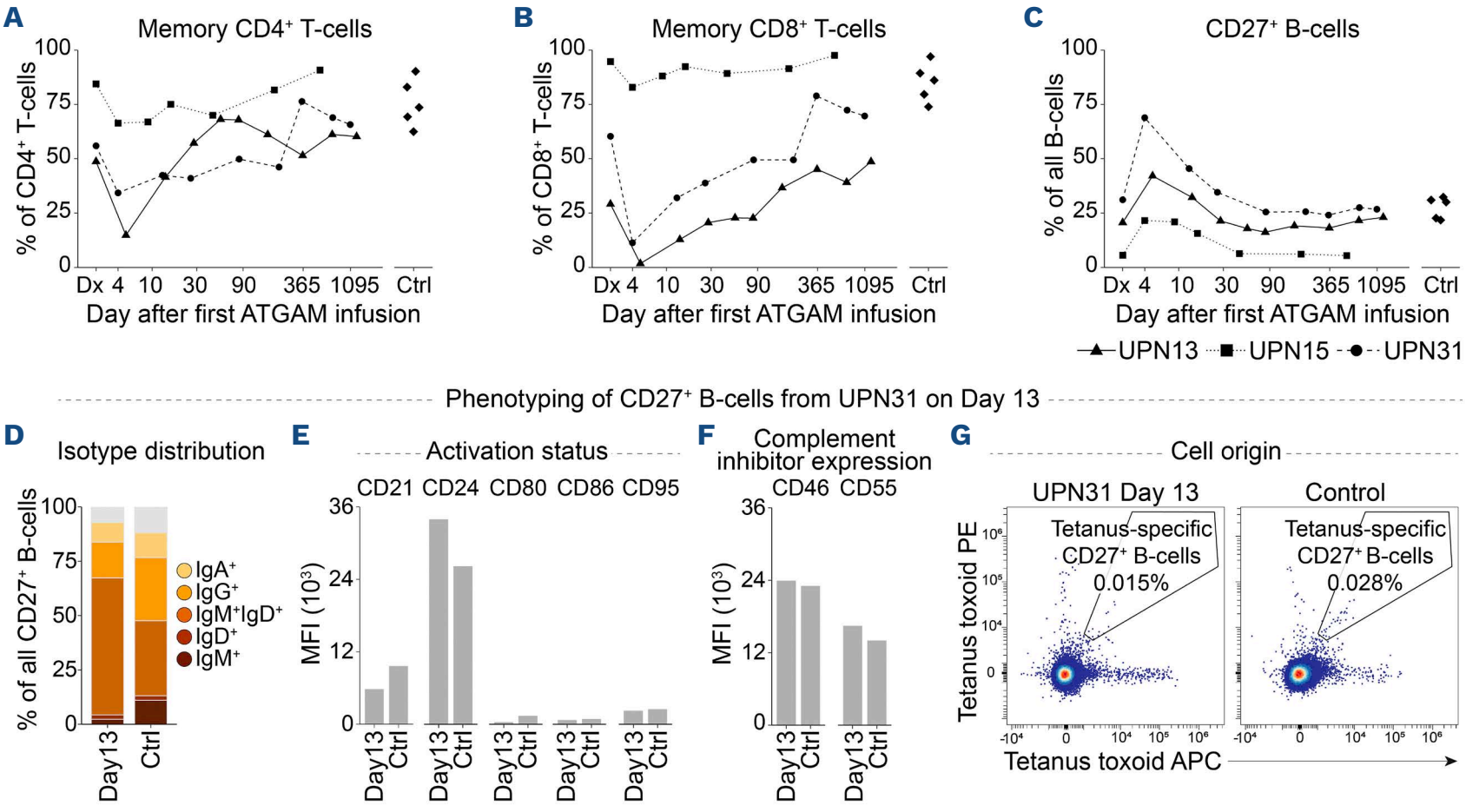

Figure 5. Dynamics of memory T cells and CD27⁺ B cells, and identity of CD27⁺ B cells, post-ATGAM. (A-C) Frequencies of memory $CD4^{+}$ T cells, memory $CD8^{+}$ T-cells or $CD27^{+}$ B-cells over time, quantified in all three aplastic anemia (AA) patients and controls. Memory T cells include central memory, effector memory and terminally differentiated effector memory T cells. (D) Isotype distribution of the $CD27^{+}$ B cells from UPN31 on day 13 after the first horse-derived anti-thymocyte globulin (ATG; ATGAM®) infusion, and the mean of 2 age-matched controls. (E) Expression of CD21, CD24, CD80, CD86 and CD95 on $CD27^{+}$ B cells from patient UPN31 on day 13, and the mean of 2 age-matched controls. Median fluorescence intensities (MFI) are shown. (F) Expression of complement inhibitors CD46 and CD55 on $CD27^{+}$ B cells from patient UPN31 on day 13, and the mean of 2 age-matched heathy controls. MFI are shown. (G) Flow cytometry plots showing the presence of tetanus toxoid-specific $CD27^{+}$ B cells in patient UPN31 on day 13, and an age-matched healthy control. $0.1x10^{6}$ $CD27^{+}$ B cells are shown per plot.

ATGAM-based immunosuppressive therapy depletes potentially pathogenic subpopulations while allowing the recovery of virus-specific lymphocytes

The rapid recovery of the T-cell compartment in the absence of proliferation, along with the persistence of pre-existing memory B cells post-ATGAM, raises the question of how profoundly ATGAM depletes the T-cell compartment. Therefore, we investigated the origin of reconstituted T cells by tracking the presence of CMV-specific CD8⁺ T cells using CMV peptide-HLA tetramers incorporated into our spectral flow cytometry panel. In one of 3 patients (UPN13), these analyses were not possible due to HLA-incompatibilities between the patient and the tetramers. In the representative patient (UPN31), we detected CMV-specific CD8⁺ T cells at diagnosis, which were no longer detectable immediately following ATGAM infusion, consistent with the observed T-cell depletion (day 4) (Figure 6A). However, CMV-specific CD8⁺ T cells were detectable from day 13 onwards, and a similar trend was observed in UPN15 (Figure 6B).

Given that our results indicate the persistence of pre-existing T and B cells post-ATGAM, we reasoned that the therapeutic effect of IST, comprising ATGAM and long-term ciclosporin, may not depend on a full immune 'reset'. Instead, it may rely on the selective depletion and suppression of pro-inflammatory CCR6⁺⁺ B cells, CCR6⁺ memory CD4⁺ T cells and KLRG1⁺ EMRA CD8⁺ T cells, which we previously identified as part of a disease-specific immune cell network.[14] These subpopulations were enriched in AA patients at diagnosis, and co-localized in bone marrow regions harboring the active immune response.[14,15] In all 3 patients, we confirmed higher frequencies of CCR6⁺⁺ B cells at diagnosis compared to controls (Figure 6C). CCR6 expression on B cells remained high immediately post-ATGAM but gradually decreased with long-term ciclosporin use, with the

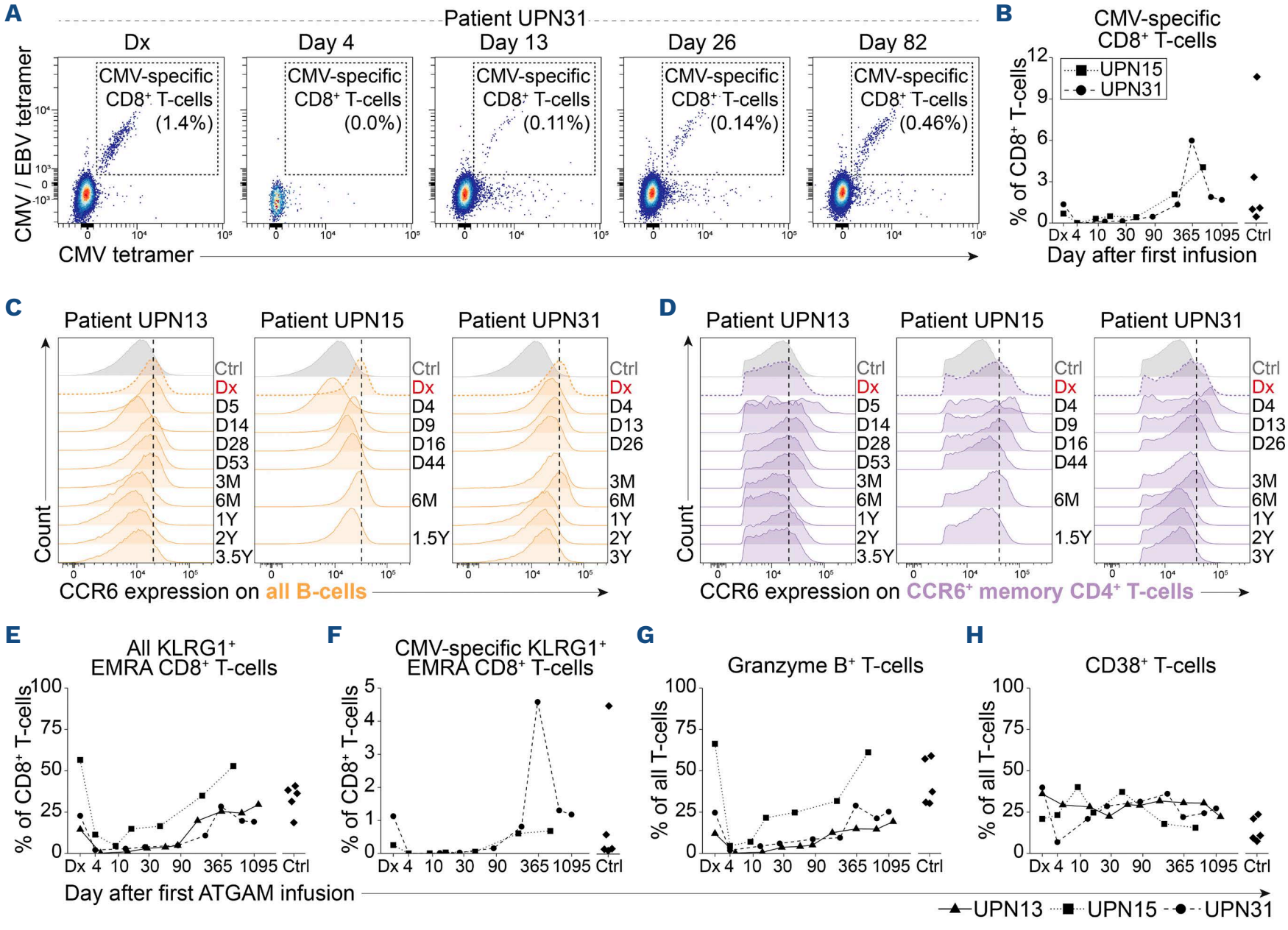

Figure 6. Effects of ATGAM on pre-existing and potentially pathogenic subpopulations. (A) Flow cytometry plots showing the presence of cytomegalovirus (CMV)-specific CD8⁺ T cells within the CD8⁺ T-cell compartment at diagnosis and after the first horse-derived anti-thymocyte globulin (ATG; ATGAM®) infusion in patient UPN31. (B) Frequencies of CMV-specific CD8⁺ T cells, quantified as a frequency of all CD8⁺ T cells in patients UPN15 and UPN31, and all controls. (C and D) Histograms showing CCR6 expression on all CD19⁺ B cells (C) or CCR6⁺ memory CD4⁺ T cells (D) in the 3 aplastic anemia (AA) patients over time following ATGAM infusion and ciclosporin treatment. (E-H) Frequencies of all KLRG1⁺ terminally differentiated effector memory (EMRA) CD8⁺ T cells, CMV-specific KLRG1⁺ EMRA CD8⁺ T cells, Granzyme B⁺ cytotoxic T cells and CD38⁺ activated T cells in all 3 AA patients over time following ATGAM infusion. EBV: Epstein-Barr virus.

strongest decrease in CCR6 expression seen more than six months post-ATGAM. CCR6 expression remained reduced after ciclosporin was discontinued (≥3 years post-ATGAM). A similar decrease in CCR6 expression on CCR6$^+$ memory CD4$^+$ T cells was observed (Figure 6D). In contrast, KLRG1$^+$ EMRA CD8$^+$ T cells were strongly depleted immediately post-ATGAM (Figure 6E), and their recovery was delayed compared to other CD8$^+$ T cells (Figure 3C). Further analysis showed that only a small fraction of these KLRG1$^+$ EMRA CD8$^+$ T cells were CMV-specific, suggesting depletion also affected potentially autoreactive T cells within this population (Figure 6F). Over time, KLRG1$^+$ EMRA CD8$^+$ T-cell frequencies returned to pre-ATGAM levels, indicating a temporary rather than a permanent depletion. A depletive effect was also observed for Granzyme B$^+$ cytotoxic T cells (Figure 6G), while expression of the activation marker CD38 remained unaffected by ATGAM plus ciclosporin (Figure 6H). These findings underscore the observation that IST results in an immediate but selective depletion of key T-cell populations by ATGAM, while other potentially pathogenic populations are reduced over several months, possibly through selective suppression by ciclosporin.

Discussion

In this study, we investigated the pharmacodynamics of first-line IST with ATGAM plus long-term ciclosporin in AA patients. Our analysis is the first to focus on active ATGAM, the fraction capable of binding human lymphocytes and mediating the immunomodulatory effects that are believed to underly its therapeutic efficacy. POPPK modeling revealed that active ATGAM exposure varies considerably among patients and tends to correlate with hematologic recovery. At high plasma concentrations, ATGAM binds T and NK cells and drastically reduces their counts *in vivo*. Paradoxically, while ATGAM also binds B cells, it does not induce their depletion but rather results in an increase in resting memory CD27$^+$ B cells in circulation. Following ATGAM infusion, immune reconstitution occurs rapidly within two weeks and is marked by the recovery of pre-existing cells alongside a selective suppression of specific pro-inflammatory subpopulations over time. Thus, the therapeutic effect of ATGAM-based IST goes beyond 'simple' lymphodepletion.

So far, ATGAM has been administered at a fixed dose per kilogram bodyweight, although its optimal dose remains unclear since its exposure-response profile has not been characterized in detail.[2,21,22] This study provides unique insight into ATGAM pharmacokinetics and offers important considerations regarding dosing. Consistent with data on rabbit-derived ATG,[23,24] we demonstrate that linear weight-based dosing causes variability in active ATGAM exposure between patients. In line with a previous report[25] that suggested a benefit of higher ATGAM exposures on relapse rates, we found that higher active ATGAM exposures tend to associate with increased neutrophil and reticulocyte counts starting 60 days post-ATGAM infusion. Although these associations did not reach statistical significance, the observed trend could be suggestive of a possible relationship between active ATGAM exposure and the timing of hematologic recovery. These findings may complement previous studies that identified patient- and disease-specific characteristics predicting response to IST, suggesting that hematologic recovery may be controlled by multiple factors.[26-32] The biological mechanism by which active ATGAM exposure may influence hematologic recovery remains unclear. In our study, active ATGAM exposure was not significantly associated with the extent or duration of T- or NK-cell depletion. Although we did not assess ciclosporin levels, their impact seems limited, given that ciclosporin dosing was concentration-controlled to a pre-specified target.[2] Interestingly, it has been reported that ATGAM can stimulate progenitor cells[33] and the release of factors regulating hematopoiesis.[13,34] Thus, higher ATGAM exposures could have a favorable effect through a stronger influence on the progenitors in the bone marrow. By applying flow cytometry, we provide a detailed description of both the short- and long-term immunological effects of ATGAM plus ciclosporin in AA patients. Although it is known that ATGAM results in less profound lymphodepletion compared to other ATG preparations,[4] our findings show that immune reconstitution occurs early post-ATGAM while active ATGAM concentrations are still detectable. This indicates that a minimal level should be exceeded for adequate lymphodepletion, and that a better understanding of the exposure-response relationship of ATGAM is needed to optimize treatment across patients. Importantly, our analyses revealed how successful IST may reshape the immune landscape to enable bone marrow recovery in AA patients. Our study, therefore, builds upon recent reports demonstrating the added value of high-dimensional single-cell techniques in deciphering the pathogenesis of AA,[14,15,35,36] and complements a comprehensive review of their application in AA.[37] Previously, using (imaging) mass cytometry on bone marrow samples from AA patients, we identified a disease-specific immune cell network of CCR6^{++} B cells, Th17-like[32,38,39] CCR6$^+$ memory CD4$^+$ T cells and KLRG1$^+$ EMRA CD8$^+$ T cells.[14,15] These immune cells were significantly enriched in AA patients at diagnosis compared to healthy donors, and showed a trend towards normalization six months after successful IST, implying a pathogenic role. In this study, we extend these findings by confirming their increased presence at diagnosis. Importantly, we further show how these cells are reduced with IST through an analysis of unique series of PBMC samples collected pre- and up to 3.5 years post-ATGAM. Our study thereby provides a more dynamic visualization of the reshaping of the immune landscape compared to previous reports that generally focused on

samples collected pre- and six months post-ATGAM.[14,15,36,39] Although the analysis included only 3 patients, it allowed for a deeper investigation beyond the major immune lineages assessed in the full cohort of 44 AA patients, and sets the stage for more widely applied longitudinal analyses in future studies. We demonstrate that successful IST depletes potentially pathogenic populations via two distinct mechanisms. Firstly, KLRG1$^+$ EMRA CD8$^+$ and CCR6$^+$ memory CD4$^+$ T cells are depleted by ATGAM. In contrast, CCR6^{++} B cells and residual T cells, including CCR6$^+$ memory CD4$^+$ T cells, gradually decrease within several months during long-term ciclosporin use. These data indicate the persistence of potentially pathogenic immune cell subpopulations post-ATGAM and could explain why long-term ciclosporin is needed to achieve durable response rates. Based on prior studies,[4,13] we expected ATGAM to bind T cells and to cause rapid but short-lived T-cell depletion. Our data confirm this effect and further reveal important differences among T-cell subpopulations. Specifically, memory T cells were more profoundly depleted than naïve T cells, suggesting that ATGAM targets cytotoxic T cells, while preserving part of the antigen-naïve T-cell repertoire that provides protection against future pathogen encounters. This effect is more pronounced among CD8$^+$ T cells compared to CD4$^+$ T cells, and remains detectable up to six months post-ATGAM, likely due to the inhibition of T-cell proliferation and differentiation by ciclosporin.[40] During this period, we observed reconstitution of CMV-specific CD8$^+$ T cells, implying that ATGAM does not result in a full immune 'reset'. Although the recovery of pre-existing cells has been described with other ATG preparations,[41] it raises questions on how successful IST eliminates potential autoreactive T cells while preserving protective immune memory. We consider three possible explanations. First, ATGAM may exert a stronger effect on autoreactive T cells compared to other memory T cells, possibly due to differences in cellular state. Similarly, it is possible that, in the absence of infections, remaining autoreactive T cells post-ATGAM may be more susceptible to ciclosporin compared to pathogenic-specific T cells due to continued antigenic triggering. Finally, it could be that ATGAM depletes memory T cells in the blood and bone marrow, while not affecting tissue-resident T cells. This would suggest that autoreactive T cells are limited to the blood and bone marrow, and that targeting these compartments alone could suffice to enable bone marrow recovery.

Since ATGAM has strong effects on T cells, it is noteworthy that our data confirm that ATGAM does not have the same effect on B cells.[13] Instead of depletion, we report a shift in the B-cell compartment, characterized by an increase in memory CD27$^+$ B cells immediately post-ATGAM infusion, which gradually normalizes within one month. These CD27$^+$ B cells comprised a heterogeneous population of both non-switched and switched memory B cells in a resting state. The CD27$^+$ B-cell population included pre-existing pathogen-specific cells as evidenced by the presence of tetanus toxoid-specific B cells and was not proliferating. Therefore, we believe that the observed increase in CD27$^+$ B cells may reflect redistribution of memory B cells from the lymphoid organs into the circulation. This could be driven by an imbalance of chemotactic factors released following T-cell apoptosis. How B cells survive ATGAM binding to their cell surface while T cells are depleted needs to be clarified in future studies. Our data revealed no increased resistance of B cells to complement-mediated lysis, nor an influence of Fc-binding. Given that ATGAM is a polyclonal antibody preparation generated against thymocytes, it is possible that ATGAM induces T-cell apoptosis by triggering T-cell activation (e.g., via anti-CD3 or TCR binding), without activating apoptotic pathways in B cells.

To conclude, we reveal active ATGAM exposure to be a clinically relevant factor influencing hematologic recovery in AA. We further demonstrate that successful IST with ATGAM plus long-term ciclosporin exerts differential effects among major lymphoid lineages, leading to selective depletion and suppression of CCR6$^+$ and KLRG1$^+$ T- and B-cell subpopulations implicated in AA pathogenesis. These findings confirm their potential pathogenicity and establish these subpopulations as a promising focus for targeted treatment.

Disclosures

No conflicts of interest to disclose.

Contributions

ESP performed laboratory experiments and pharmacokinetic modelling, analyzed and interpreted the data, and wrote the first draft of the manuscript; CRP and SMG performed laboratory experiments; EHMvE and JMG performed laboratory experiments and interpreted the data; SV performed laboratory experiments; DJARM performed pharmacokinetic modelling, interpreted the data, conceptualized the study and supervised the project; REMT and FK interpreted the data; CJMH interpreted the data, recruited patients and collected samples; MHMH interpreted the data and supervised the project; JM-LT interpreted the data, recruited patients and collected samples, conceptualized the study and supervised the project. All authors critically reviewed the manuscript.

Acknowledgments

We thank the Laboratory for Special Hematology of the Leiden University Medical Center for processing all plasma samples. Furthermore, we thank Anja Jansen-Hoogendijk of the Department of Pediatrics of the Leiden University Medical Center for sharing her expertise on measuring active ATG concentrations in patient plasma. Flow cytometry was performed at the Flow Cytometry Core Facility of the Leiden University Medical Center.

Funding
This work was supported by a research grant from Dioraphte Foundation.

Data-sharing statement
Pharmacokinetic and spectral flow cytometry data acquired in this study are available from the corresponding author upon reasonable request.

References

1. Young NS. Aplastic anemia. N Engl J Med. 2018;379(17):1643-1656.
2. Kulasekararaj A, Cavenagh J, Dokal I, et al. Guidelines for the diagnosis and management of adult aplastic anaemia: a British Society for Haematology guideline. Br J Haematol. 2024;204(3):784-804.
3. Halkes CJ, Veelken H, Falkenburg JH. Horse versus rabbit antithymocyte globulin in aplastic anemia. N Engl J Med. 2011;365(19):1842-1843.
4. Scheinberg P, Nunez O, Weinstein B, et al. Horse versus rabbit antithymocyte globulin in acquired aplastic anemia. N Engl J Med. 2011;365(5):430-438.
5. Peffault de Latour R, Kulasekararaj A, Iacobelli S, et al. Eltrombopag added to immunosuppression in severe aplastic anemia. N Engl J Med. 2022;386(1):11-23.
6. Genestier L, Fournel S, Flacher M, Assossou O, Revillard JP, Bonnefoy-Berard N. Induction of Fas (Apo-1, CD95)-mediated apoptosis of activated lymphocytes by polyclonal antithymocyte globulins. Blood. 1998;91(7):2360-2368.
7. Mohty M. Mechanisms of action of antithymocyte globulin: T-cell depletion and beyond. Leukemia. 2007;21(7):1387-1394.
8. Elliott JF, Lin Y, Mizel SB, Bleackley RC, Harnish DG, Paetkau V. Induction of interleukin 2 messenger RNA inhibited by cyclosporin A. Science. 1984;226(4681):1439-1441.
9. Heidt S, Roelen DL, Eijsink C, et al. Calcineurin inhibitors affect B cell antibody responses indirectly by interfering with T cell help. Clin Exp Immunol. 2010;159(2):199-207.
10. Popow I, Leitner J, Grabmeier-Pfistershammer K, et al. A comprehensive and quantitative analysis of the major specificities in rabbit antithymocyte globulin preparations. Am J Transplant. 2013;13(12):3103-3113.
11. Bourdage JS, Hamlin DM. Comparative polyclonal antithymocyte globulin and antilymphocyte/antilymphoblast globulin anti-CD antigen analysis by flow cytometry. Transplantation. 1995;59(8):1194-1200.
12. Raefsky EL, Gascon P, Gratwohl A, Speck B, Young NS. Biological and immunological characterization of ATG and ALG. Blood. 1986;68(3):712-719.
13. Feng X, Scheinberg P, Biancotto A, et al. In vivo effects of horse and rabbit antithymocyte globulin in patients with severe aplastic anemia. Haematologica. 2014;99(9):1433-1440.
14. Pool ES, Kooy-Winkelaar Y, van Unen V, et al. Mass cytometric analysis unveils a disease-specific immune cell network in the bone marrow in acquired aplastic anemia. Front Immunol. 2023;14:1274116.
15. Pool ES, Luk SJ, Ijsselsteijn ME, et al. Imaging mass cytometry reveals the order of events in the pathogenesis of immune-mediated aplastic anemia. Blood. 2025;146(8):951-963.
16. Tjon JM-L, Hussen-Dassen LGMv, Nur E, et al. Dutch guidelines for diagnostics and treatment of acquired aplastic anemia in adults. Nederlands Tijdschrift voor Hematologie. https://publicatie.hematologienederland.nl/richtlijnen/verworven-aplastische-anemie-bij-volwassenen-2/ Accessed February 25, 2026.
17. Rebello P, Hale G. Pharmacokinetics of CAMPATH-1H: assay development and validation. J Immunol Methods. 2002;260(1-2):285-302.
18. Van Gassen S, Callebaut B, Van Helden MJ, et al. FlowSOM: using self-organizing maps for visualization and interpretation of cytometry data. Cytometry A. 2015;87(7):636-645.
19. Comets E, Lavenu A, Lavielle M. Parameter estimation in nonlinear mixed effect models using saemix, an R Implementation of the SAEM algorithm. J Stat Softw. 2017;80(3):1-41.
20. Pfizer. ATGAM (anti-thymocyte globulin (equine) sterile solution) Perscribing Information. https://labeling.pfizer.com/ShowLabeling.aspx?id=12213 Accessed 8 Jan 2025.
21. Scott A, Morris K, Butler J, Mills AK, Kennedy GA. Treatment of aplastic anaemia with lower-dose anti-thymocyte globulin produces similar response rates and survival as per standard dose anti-thymocyte globulin schedules. Intern Med J. 2016;46(10):1198-1203.
22. Young N, Griffith P, Brittain E, et al. A multicenter trial of antithymocyte globulin in aplastic anemia and related diseases. Blood. 1988;72(6):1861-1869.
23. Admiraal R, van Kesteren C, Jol-van der Zijde CM, et al. Population pharmacokinetic modeling of Thymoglobulin® in children receiving allogeneic-hematopoietic cell transplantation: towards improved survival through individualized dosing. Clin Pharmacokinet. 2015;54(4):435-446.
24. Oostenbrink LVE, Von Asmuth EGJ, Jol-van der Zijde CM, et al. Anti-T-lymphocyte globulin exposure is associated with acute graft-versus-host disease and relapse in pediatric acute lymphoblastic leukemia patients undergoing hematopoietic stem cell transplantation: a multinational prospective study. Haematologica. 2024;109(9):2854-2863.
25. Walter J, Rolles B, Schumacher Y, et al. Analysis of the impact of body mass index (BMI) on the durability of response in patients with aplastic anemia treated with weight-adjusted horse anti-thymocyte globulin (hATG). Blood. 2023;142(Suppl 1):5641.
26. Scheinberg P, Wu CO, Nunez O, Young NS. Predicting response to immunosuppressive therapy and survival in severe aplastic anaemia. Br J Haematol. 2009;144(2):206-216.
27. Yoshizato T, Dumitriu B, Hosokawa K, et al. Somatic mutations and clonal hematopoiesis in aplastic anemia. N Engl J Med. 2015;373(1):35-47.
28. Narita A, Muramatsu H, Sekiya Y, et al. Paroxysmal nocturnal hemoglobinuria and telomere length predicts response to immunosuppressive therapy in pediatric aplastic anemia. Haematologica. 2015;100(12):1546-1552.
29. Zhao X, Zhang L, Jing L, et al. The role of paroxysmal nocturnal hemoglobinuria clones in response to immunosuppressive therapy of patients with severe aplastic anemia. Ann Hematol. 2015;94(7):1105-1110.

30. Sugimori C, Chuhjo T, Feng X, et al. Minor population of CD55-CD59- blood cells predicts response to immunosuppressive therapy and prognosis in patients with aplastic anemia. Blood. 2006;107(4):1308-1314.
31. Zaimoku Y, Patel BA, Kajigaya S, et al. Deficit of circulating CD19(+) CD24(hi) CD38(hi) regulatory B cells in severe aplastic anaemia. Br J Haematol. 2020;190(4):610-617.
32. Kordasti S, Costantini B, Seidl T, et al. Deep phenotyping of Tregs identifies an immune signature for idiopathic aplastic anemia and predicts response to treatment. Blood. 2016;128(9):1193-1205.
33. Huang AT, Mold NG, Zhang SF. Antithymocyte globulin stimulates human hematopoietic progenitor cells. Proc Natl Acad Sci U S A. 1987;84(16):5942-5946.
34. Nimer SD, Golde DW, Kwan K, Lee K, Clark S, Champlin R. In vitro production of granulocyte-macrophage colony-stimulating factor in aplastic anemia: possible mechanisms of action of antithymocyte globulin. Blood. 1991;78(1):163-168.
35. Lundgren S, Huuhtanen J, Keranen M, et al. Single-cell analysis of aplastic anemia reveals a convergence of NK and NK-like CD8(+) T cells with a disease-associated TCR signature. Sci Transl Med. 2025;17(787):eadl6758.
36. Wu Z, Gao S, Feng X, et al. Human autoimmunity at single cell resolution in aplastic anemia before and after effective immunotherapy. Nat Commun. 2025;16(1):5048.
37. Wu Z, Young NS. Single-cell genomics in acquired bone marrow failure syndromes. Blood. 2023;142(14):1193-1207.
38. de Latour RP, Visconte V, Takaku T, et al. Th17 immune responses contribute to the pathophysiology of aplastic anemia. Blood. 2010;116(20):4175-4184.
39. Kordasti S, Marsh J, Al-Khan S, et al. Functional characterization of CD4+ T cells in aplastic anemia. Blood. 2012;119(9):2033-2043.
40. Jenkins MK, Schwartz RH, Pardoll DM. Effects of cyclosporine A on T cell development and clonal deletion. Science. 1988;241(4873):1655-1658.
41. Havenith SH, Remmerswaal EB, Bemelman FJ, et al. Rapid T cell repopulation after rabbit anti-thymocyte globulin (rATG) treatment is driven mainly by cytomegalovirus. Clin Exp Immunol. 2012;169(3):292-301.